

# Linking Electricity and Air Quality Models by Downscaling: Weather-Informed Hourly Dispatch of Generation

## Accounting for Renewable and Load Temporal Variability Scenarios

Authors: Shen Wang<sup>\*1,2</sup>, Hanzhi Wang<sup>1</sup>, J. Hugh Ellis<sup>1</sup>, and Benjamin F. Hobbs<sup>1</sup>

1. Dept. of Environmental Health & Engineering, Johns Hopkins University, Baltimore, MD, 21212, USA

2. *Centre for Energy and Environmental Policy Research, Massachusetts Institute of Technology, Cambridge, MA 02139, USA*

## Abstract

National models of the electric sector typically consider a handful of generator operating periods per year, while pollutant fate and transport models have an hourly resolution. We bridge that scale gap by introducing a novel fundamentals-based temporal downscaling method (TDM) for translating national or regional energy scenarios to hourly emissions. Optimization-based generator dispatch is used to account for variations in emissions stemming from weather-sensitive power demands and wind and solar generation. TDM is demonstrated by downscaling emissions from the electricity market module in the National Energy Model System (NEMS). As a case study, we implement the TDM in the Virginia-Carolinas region and compare its results with traditional statistical downscaling used in the Sparse Matrix Operator Kernel Emissions (SMOKE) processing model. We find that the TDM emissions profiles respond to weather, and that nitrogen oxide emissions are positively correlated with conditions conducive to ozone formation. In contrast, SMOKE emissions time series, which are rooted in historical operating patterns, exhibit insensitivity to weather conditions and potential biases, particularly with high renewable penetration and climate change. Relying on SMOKE profiles can also obscure variations in emission patterns across different policy scenarios, potentially downplaying their impacts on power system operations and emissions.

## Synopsis

23 This research proposes a novel downscaling methodology to link macro-energy system models and air  
24 quality models accounting for projecting power emissions changes due to renewable technology innovation,  
25 weather-informed system operation changes and load variability.

**Keywords:** power systems, power emission, energy transitions, emission projection

27 1. Introduction

28 An oft-stated objective of policies and strategies to combat climate change is the achievement of a net-  
29 zero emission economy by the mid-21st century. To limit global warming to 1.5°C, the Paris Agreement  
30 set targets for greenhouse gas emissions to decline 45% at least before 2030 and to reach net-zero by 2050

\* Corresponding author contact: [swang187@alumni.jh.edu](mailto:swang187@alumni.jh.edu)

31 worldwide [1],[2]. In the US, President Biden has set an ambitious national goal of achieving a carbon  
32 pollution-free power sector by 2035 and a net zero emissions economy before 2050 [3]. Because the energy  
33 sector is responsible for 73% of greenhouse gas emissions globally, decarbonizing the energy system is the  
34 emphasis of policy [4],[5]. Various clean energy transition “pathways” and “roadmaps” have been proposed  
35 and widely discussed by government, academia, and industry [4],[6]–[8]. Decarbonizing the electricity sec-  
36 tor is often the focus of these plans, not only because power production is responsible for 25% of world-  
37 wide emissions [9], but also because electrifying the transport and building sectors is viewed as key to their  
38 decarbonization.

39 Recently, the social impacts of the energy transition have gained the attention of the public, policy  
40 makers, and researchers, with a focus on effects such as air quality, public health, energy equity, environ-  
41 mental justice, and labor markets [10-16]. Analyzing these impacts requires the integration of different  
42 modeling tools from various disciplines, such as long-term macro-energy system models/integrated assess-  
43 ment models [16],[17], air quality models [18],[19], dose-response models for health impacts [21], and  
44 aggregated sectoral micro-economic models (i.e., power, transportation, and building) [22-24], among oth-  
45 ers. However, it is often difficult to coordinate the inputs and outputs of these models to provide an inte-  
46 grated look at the multiple impacts of policy as those models are usually implemented on different spatial  
47 and temporal scales. In the temporal dimension, for instance, most macro-energy systems or climate models  
48 reduce computational complexity by decreasing the temporal resolution of the data used. Instead of 8760  
49 hours/yr, the National Energy Modeling System (NEMS) model uses nine time-block periods per year for  
50 its load inputs and electricity outputs, while the Regional Energy Deployment System (ReEDS) model  
51 applies an aggregated seventeen time-blocks to represent the within-year distribution of loads [10, 11].  
52 Thus, the rough output of such a model cannot be directly used by air quality models that require highly  
53 resolved temporal data (i.e., an hourly time step) as inputs. Therefore, (temporal) downscaling techniques  
54 are needed to link aggregated system models with air quality models.

55 A downscaling method usually takes an aggregate spatial or temporal forecast of climate, economic, or  
56 other variables as an input (or “predictor”), and produces a more detailed and disaggregated scenario of  
57 those variables or other variables that are affected by those inputs. Current downscaling methods can be  
58 categorized into statistical [26-32], dynamic [33-36], and fundamentals-based [37, 39] approaches. We re-  
59 view the existing literature associated with each approach in Support Information (SI) Section 1, focusing  
60 on applications to electricity demand, generation, and emissions downscaling.

61 However, existing downscaling methods have limitations in capturing the effects of long-term (beyond  
62 10-15 years) changes in power generation mixes or climate (e.g., average temperatures). Such factors,  
63 which can significantly impact the amount and timing of power emissions during energy transitions, are  
64 not well represented or ignored. In the case of statistical approaches, the assumption that the statistical

65 relationship built using historical or current system data will still be valid for the future system could fun-  
66 damentally limit downscaling projections to just the next handful of years rather than the decades covered  
67 by energy transition scenarios. Meanwhile, the precision of temporal downscaling is restricted by the phys-  
68 ical model used. For instance, the temporal resolution of GCM (General Circulation Model) results  
69 downscaled using RCMs (Regional Circulation Models) is often in 6-hour time steps, which is not detailed  
70 enough to represent the diurnal operation of a power system and its associated emissions [33]. In addition,  
71 a fundamentals-based method was used by Loughlin et al. [39], who proposed an SCC-mapped<sup>1</sup> grow-in-  
72 place (GIP) method to link MARKAL and SMOKE-CMAQ (Sparse Matrix Operator Kernel Emissions -  
73 Community Multi-scale Air Quality) modeling frameworks to project and simulate both the location and  
74 time series of energy sector emissions. A combined GIP and SMOKE (GIP-SMOKE) model does temporal  
75 downscaling by converting annual emissions into hourly emissions through its default allocation fac-  
76 tors/temporal profiles, which may consider the pattern differences between day and night, weekdays and  
77 weekends, and months or seasons, but have the shortcoming of being assumed to not change in future years.

78 Therefore, better downscaling methods are desirable to generate more accurate emission profiles that  
79 can represent how temporal emissions patterns evolve over future years in response to renewable invest-  
80 ment, changed power system operations, and variable weather conditions. Firstly, an improved downscaling  
81 approach should be able to capture changing net-load patterns (gross load less renewable generation, e.g.,  
82 the so-called Duck Curve of the California power system<sup>2</sup>) and timing of demand peaks. These variations  
83 are expected to create a greater need for more flexible ramping of fossil-fueled thermal plants to maintain  
84 system reliability, inevitably altering the corresponding amount and timing of power sector emissions. Sec-  
85 ond, the new approach should account for climate change which might affect future power system reliability  
86 by magnifying the impacts of weather on demand variability [42], [43]. Climate change can also reduce or  
87 increase the generation of renewable energy, and warming reduces the effective capacity and Carnot effi-  
88 ciency of thermal plants [42, 44-46]. These shifts deserve careful attention when assessing the impacts of  
89 power emissions on air quality and public health, as the effectiveness of power emission reduction can be  
90 significantly influenced by changes in emissions distribution over the year and their correlations with syn-  
91 optic conditions [47]. For instance, elevated NO<sub>x</sub> emissions during high temperature/high demand days may  
92 coincide with conditions favorable for ozone formation [40]. However, the temporal profiles in SMOKE  
93 generally do not capture these correlations because those profiles are designed to represent historical

---

<sup>1</sup>The Source Classification/Category Codes (SCCs) system was developed by US EPA to classify different types of activities that generate emissions [41]. Each SCC is given to a unique source category-specific process or function that emits air pollutants.

<sup>2</sup> The duck curve is a graph shows the difference between electricity demand and solar energy production over a day. It was devised by the CAISO to illustrate an aspect of challenges that renewable energy poses to system flexibility.

94 average conditions and do not represent their day-to-day random variability. As a result, SMOKE may  
95 underestimate peak generation emissions while overpredicting emissions during other time periods [48]. .  
96 [The latter are often focused instead on projecting long-term changes in siting patterns due to large-scale](#)  
97 [fossil retirements and renewable investments, and require national downscaling of results from NEMS and](#)  
98 [other national models.](#)

99 In this paper, we focus on developing temporal downscaling methods for electricity systems that can  
100 more precisely represent impacts of renewable energy growth and other system changes on the level and  
101 variability of power emissions accounting for economic, technical, and climate drivers. The proposed  
102 method is intended to combine the advantages of both statistical downscaling and dynamic downscaling.  
103 Some simple drivers like temperature, wind speed, and solar radiation are processed and downscaled by  
104 statistical methods. Our method then applies optimization to simulate electric generator operations on an  
105 hourly times scale using those statistically downscaled meteorological variables, [based on the locations of](#)  
106 [existing and new power plant projected using](#) a site-and-grow (SAG) [49] spatial downscaling method.  
107 [SAG is designed to model the spatial distribution of changes in generator locations based on modeling of](#)  
108 [generator retirements and new plant construction. SAG constrains overall future installed capacity mixes](#)  
109 [using future scenarios from national or regional energy models, and chooses where to site new facilities](#)  
110 [based either on statistical methods reflecting past siting patterns \[40\] or optimization methods that account](#)  
111 [for transmission, water, land availability, and other factors affecting siting, especially the amount and dis-](#)  
112 [tribution of wind and solar resources in the case of renewable generators \[49\]. The advantage of optimiza-](#)  
113 [tion-based SAG models is that they can account for siting costs and requirements for new generation tech-](#)  
114 [nologies that can differ significantly from drivers of siting decisions for traditional thermal generators.](#)

115 The resulting temporally downscaled emissions are expected to anticipate how changes in technology,  
116 policy, and climate drivers affect when and how facilities are operated on an hourly scale. Using this new  
117 method, we are able to address the following research questions: 1) *How do hourly emission distributions*  
118 *from thermal plants vary and correlate with meteorological conditions in the context of climate change,*  
119 *and how do they compare to traditional methods that don't account for meteorological variability?*, and 2)  
120 *How do hourly distributions of power sector emissions compare under alternative policy and technology*  
121 *scenarios, accounting for the response of emissions to the penetration of wind and solar energy and its*  
122 *contributions to net-load variations?* The proposed hybrid statistical-SAG-temporal optimization-based  
123 method for temporal and spatial emissions downscaling is a novel approach in that this is the first time that  
124 a downscaling method considers hourly operations of a power system in response to renewable energy  
125 penetration and climate drivers over a multi-decadal time scale.

126 The rest of the paper is organized as follows. Section 2 introduces the proposed temporal downscaling  
127 methodology and case study assumptions. Section 3 shows the numerical case study for the SERC

128 Virginia/Carolina (SRVC) region in the year 2050<sup>1</sup> under several energy transition scenarios. Section 4  
129 discusses implications of these results and recommends future research directions.

## 130 **2 Methods**

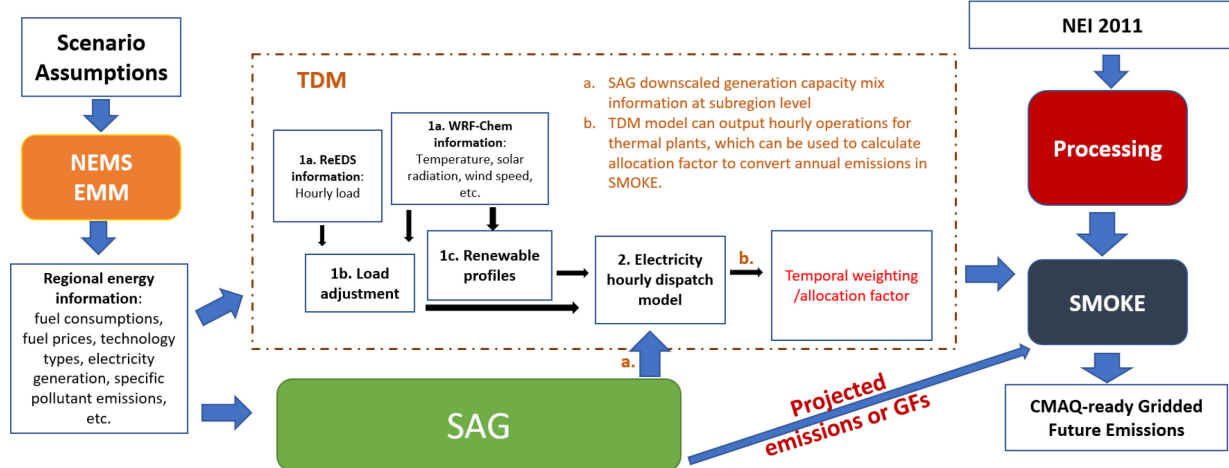
### 131 **2.1 Temporal Downscaling Model**

132 The proposed temporal downscaling model (TDM) disaggregates energy outputs from a scale of multi-  
133 hour time blocks (several blocks per year) yielded by a national or regional aggregated electricity model to  
134 an hourly scale while accounting for how power systems will be operated in the future under significant  
135 renewable penetration as well as varying meteorological conditions under climate change and an assumed  
136 policy scenario. Specifically, the TDM is designed to link the NEMS model and the **SMOKE**-CMAQ model  
137 but is not limited to these two particular models. It can be extended to downscale emissions from the electric  
138 power component of any other macro-energy system model, integrated assessment model, or other time-  
139 aggregated models of power system operations for use in any pollutant fate and transport model.

140 Here, we describe the specific steps of TDM, assuming that the locations and sizes of electric generators  
141 for some future scenario have been provided by the NEMS-SAG method [49]. The TDM comprises two  
142 major steps as shown in Figure 1, each being explained in detail in SI Sections 2.1-2.2, respectively. (Note  
143 that in our application, the execution of NEMS and SMOKE was done by collaborators on other research  
144 teams, while our contributions are the SAG-TDM downscaling components of the overall process). The  
145 first step addresses net-load adjustments which will affect hourly MW demands (loads) and potential MW  
146 generation by renewables (solar, wind). It is made up of three substeps (SI Sections 2.1.1-2.1.3, respec-  
147 tively). The first substep is the development of hourly load and meteorological scenarios simulated from  
148 external models (Step 1a. ReEDS and WRF model, Fig. 1). The second substep consists of load adjustments  
149 (Step 1b, Fig. 1), and the third step is a simulation of potential renewable profiles (Step 1c, Fig 1). The last  
150 two substeps predict and simulate future hourly load and renewable production profiles consistent with  
151 patterns of statistically downscaled meteorological variables. These profiles are then used as inputs in the  
152 second step of TDM (Step 2, Fig. 1).

---

<sup>1</sup> The year 2050 scenario is selected as a long-term transition case study, which is furthest forecasting year under the used NEMS version. The proposed framework can be also used for the other short and intermediate years such as 2030 and 2040, and even longer term 2100 if meteorological data and energy projection information are available.



153

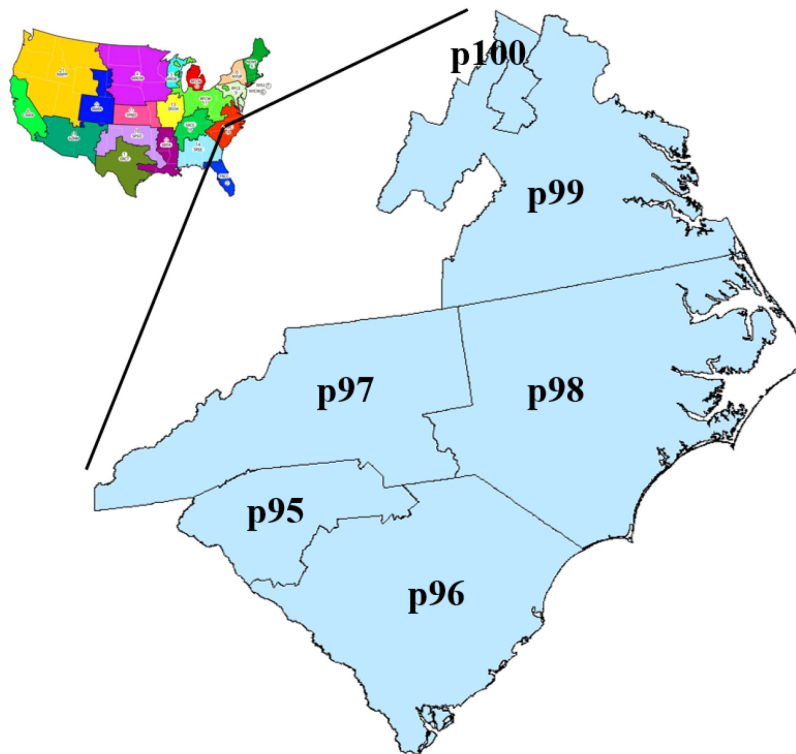
154 Figure 1. Schematic of methodology linkages within the two-step TDM framework

155

156 The core of the second step is an optimization-based hourly electricity dispatch model that determines  
 157 hourly generation from each generation type in each subregion (and ultimately power plant) in the model,  
 158 while matching the aggregate temporal profile of such generation from the national or regional aggregate  
 159 model (here, NEMS). The detailed notation and formulations of the model can be found in SI Section 2.2.  
 160 The power flows among NEMS' EMM regions by load block are solved by the NEMS model and are  
 161 therefore used in the TDM as "boundary conditions" for its downscaling procedure. Within each EMM  
 162 region, the transmission lines and subregions are represented as pipe-and-bubbles. Security constraints  
 163 among subregions, which account for the need to limit flows to less than some multiple of the thermal  
 164 capacity of transmission lines because of possible line outage contingencies are represented by a derated  
 165 transmission capacity method, which is a common approach of large systems [50]. Resistance losses be-  
 166 tween regions are disregarded, but more general formulations could calculate losses as dependent on volt-  
 167 age, power line length, and amount of flow. Unit commitment constraints on generator dispatch (e.g., ramp  
 168 rates, start-ups, or minimum output levels) are not modeled, consistent with NEMS, but could also be in-  
 169 corporated if desired. The structure of this optimization-based electricity model resembles traditional pro-  
 170 duction cost models, with two important exceptions. One is that our model also includes constraints that  
 171 require that certain energy outputs of an aggregate model (here, NEMS) be matched (namely, the sum over  
 172 TDM hourly dispatched generation in time block equals the total generation in that NEMS time block).  
 173 Second, the TDM optimization model includes more than the usual amount of detail on temporal variations  
 174 in resource availability and load, and their correlations, because the timing and amount of generation and  
 175 emissions from thermal generation are closely coupled and influenced by the joint distribution of wind and  
 176 solar output and loads, and these effects depend strongly on the exact generation mix associated with the  
 177 energy transition scenario being considered [51], [52].

178 **2.2 Case Study Assumptions**

179 As a case study, we implemented the TDM to downscale NEMS outputs in 2050 in the SRVC region  
180 (Figure 2). Results for other years from NEMS could be downscaled similarly using appropriate inputs.  
181 Based on a power plant and demand location model derived using the SAG model [49], we downscale  
182 energy (MWh) generation projections (by fuel type, technology type, time block, and sub-region) from a  
183 scale of nine NEMS time-blocks per year to 8760 hours per year (Section 3.1). Then we convert the hourly  
184 generation scenario into chronological emissions profiles which we use to modify the basic emission pro-  
185 files in [SMOKE](#)-CAMQ [18],[54].



186

187 Figure 2. Map of six ReEDS balancing areas (p95-p100) comprising the NEMS SRVC (SERC Relia-  
188 ability Corporation, Virginia and Carolinas) region

189 The inputs for this downscaling method are of four types: 1) a meteorological scenario of hourly tem-  
190 peratures, cloudiness, and wind speeds (disaggregated to subregion); 2) assumed locations of generation  
191 capacity by subregion (from either the SAG method or the more traditional GIP method [49]) with a multi-  
192 state region for a future scenario year, 3) energy generation by sub-period (NEMS' nine time-blocks in our  
193 case), and 4) local siting or emissions policies that impact dispatch. The outputs are hourly energy and  
194 pollutant emissions, in particular: 1) Hourly electricity demand and generation from all generation types  
195 (including variable renewables) in each subregion that are consistent with assumed hourly weather, as well  
196 as 2) Hourly emissions (especially SO<sub>2</sub>, NO<sub>x</sub>) by generator type and subregion. After downscaling each

197 subregion's chronological emissions further to individual point sources (e.g., by assuming an allocation in  
198 proportion to the capacity of each source present in a point source emissions inventory), those emissions  
199 can then be input into an air pollution fate and transport model such as the CMAQ system.

200 Our application repeats this process for each of four aggregate energy and emission scenarios from  
201 NEMS model:

- 202 • A base case or reference scenario uses AEO 2017 scenario, without the Obama administration  
203 Clean Power Plan [54] (scenario refnocpp),
- 204 • Abundant natural gas resources (scenario highNG) [55],
- 205 • High electric vehicle penetration (scenario highEV) [56], and
- 206 • High building energy efficiency (scenario highEE) [57].

207 The required additional information on subregional transmission, hourly load profiles, and renewable  
208 sources originate from the ReEDS database [58]. This downscaled emission information will be, by defini-  
209 tion of the methodology, consistent with NEMS totals by region and by load block (nine demand blocks  
210 per year). Finally, we compare the TDM downscaled hourly emissions with the downscaled hourly emis-  
211 sions from [SMOKE](#)'s output in terms of temporal variation and O<sub>3</sub> formation implications for each of the  
212 scenarios (Sections 3.2 - 3.4).

213 Emissions policies are key assumptions that affect the results of downscaling analyses, and are reflected  
214 either in the boundary conditions imposed on the downscaling, or the downscaling process itself. Assump-  
215 tions about federal or regional policies (such as seasonal NO<sub>x</sub> or annual SO<sub>2</sub> caps or the Regional Green-  
216 house Gas Initiative) constrain solutions of the aggregate energy models that define boundary conditions  
217 for downscaling, such as total emissions by jurisdiction or season. Downscaling method then enforces those  
218 boundary conditions so that the disaggregated emissions are consistent with the aggregate model solutions  
219 and the federal policies they reflect. However, many states impose their own specific emissions policies  
220 that should be reflected in downscaling procedures. Examples include state or local CO<sub>2</sub> targets or caps on  
221 criterion pollutants within non-attainment areas. In our case study, all emissions are incorporated in the  
222 boundary conditions defined by NEMS, but such limits on timing or location of local emissions could  
223 readily be included.

224 In general, there exist important uncertainties that should be recognized when using emission downscal-  
225 ing methods. Some of these are broad federal policy, economic, and technology uncertainties that impact  
226 mixes of generation investment and their emissions rates. These are best reflected in sensitivity analyses of  
227 the national or regional models whose aggregate results are the boundary conditions that constrain the total  
228 investment and energy generation by type within the region being studied. Other uncertainties, such as  
229 state or local land use and climate policies that influence the generator siting and operations, should be  
230 considered by downscaling under a range of assumptions about those policies to assess if the resulting

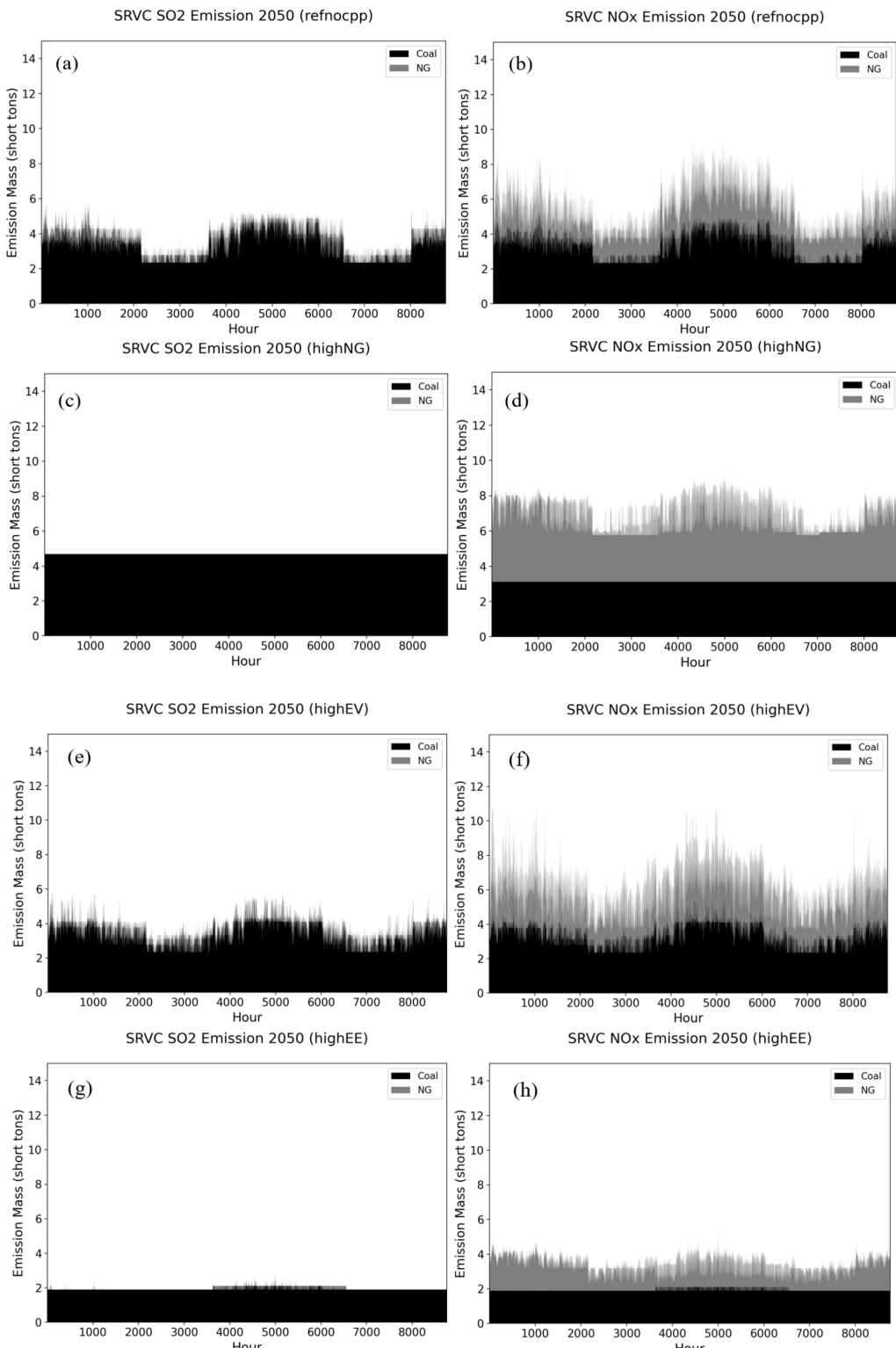
231 emissions patterns change in ways that could have significant implications for health or other impacts. For  
232 conciseness, this case study does not include such sensitivity analyses.

## 233 **3 Results**

### 234 **3.1 Hourly Generation Dispatch and Emission Profiles**

235 The scenario-by-scenario NEMS-SAG projected and downscaled generation capacity mixes are shown  
236 in Figure S8 in the SI. In this subsection, given the projected 2050 systems, we present TDM downscaled  
237 and optimized SRVC power system hourly operation under four scenarios (Figure S9. a-d). The figure  
238 reveals that nuclear, coal, natural gas, and solar energy are the primary resources meeting electricity de-  
239 mands in SRVC. In the refnocpp scenario, most of the coal and nuclear power plants operate as baseload  
240 generators, while coal was called upon occasionally during peak hours. A significant amount of solar pro-  
241 duction resulted in gas plants cycling more frequently to meet demand when insufficient solar energy was  
242 available. In the highNG case, gas plants dominate power generation instead, accounting for over 50% of  
243 total electricity production, leading to changes in coal plant operations which in that case only serve as  
244 baseload generators. The operation patterns in the highEE scenario were similar to those in the refnocpp  
245 case, but with more fluctuations during peak periods due to EV charging. Coal plant operations also changed  
246 in the highEE scenario due to reductions in overall electricity demand. By considering weather-dependent  
247 load and renewable variations, the TDM downscaling method can precisely and quantitatively assess how  
248 different energy transition scenarios affect emissions timing and amounts by capturing operating interac-  
249 tions of different resources in a quantitative manner.

250 As shown in Figure 3, temporal variations in thermal plant operation strongly affect power emissions  
251 profiles, which are the SO<sub>2</sub> and NO<sub>x</sub> hourly emission profiles projection in 2050 in the various scenarios.  
252 The emissions are calculated based on the MWh operation of thermal plants multiplied by corresponding  
253 emissions factors. The SO<sub>2</sub> profile is driven by the timing of coal combustion, while variations in NO<sub>x</sub> result  
254 from the operations of both coal and natural gas plants. Emission profiles also exhibit seasonal trends, with  
255 higher emissions occurring in summer or winter due to increased cooling and heating demands, respec-  
256 tively. In contrast, emissions in spring or fall tend to be lower. The diurnal pattern shows that there are more  
257 fluctuations in NO<sub>x</sub> during peak hours compared to SO<sub>2</sub>, reflecting the flexible operation of gas plants  
258 relative to coal plants and their interactions with solar production.



260  
261 Figure 3. Hourly power emissions in region SRVC under different 2050 scenarios (a. Refnocpp SO<sub>2</sub>; b.  
262 Refnocpp NO<sub>x</sub>; c. HighNG SO<sub>2</sub>; d. HighNG NO<sub>x</sub>; e. HighEV SO<sub>2</sub>; f. HighEV NO<sub>x</sub>; e. HighEE SO<sub>2</sub>; f.  
263 HighEE NO<sub>x</sub>)  
264

265 Differences in generation mix and location among scenarios also lead to distinct power system operations  
266 and corresponding emission profiles. For instance, in the highNG and highEE scenarios, the emissions  
267 of SO<sub>2</sub> from coal facilities remain relatively constant over time due to their baseload mode of operation.  
268 This pattern differs from the other scenarios, in which coal generates more power, expanding to include  
269 both baseload and cycling roles. Furthermore, the NO<sub>x</sub> emission profile in the highEE scenario demonstrates  
270 less fluctuation over the seasons compared to the other three scenarios. This is due to the lower demand and  
271 lower investment in new power resources in that scenario, especially wind and solar, which reduce the  
272 overall variability of net loads faced by fossil units. Thus, the TDM approach effectively captures emission  
273 variations arising from different power system configurations and operations across different energy transi-  
274 tion scenarios.

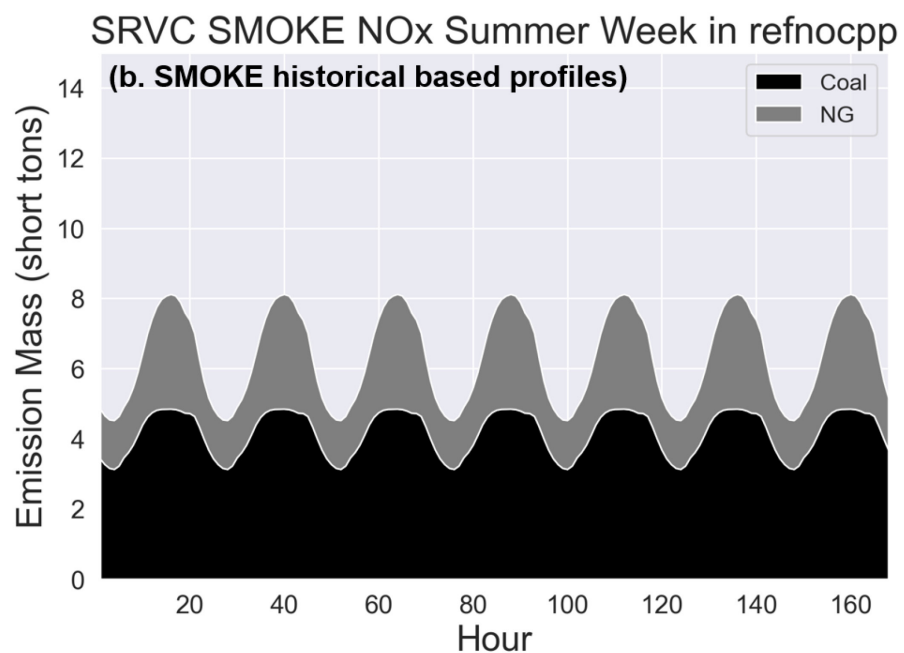
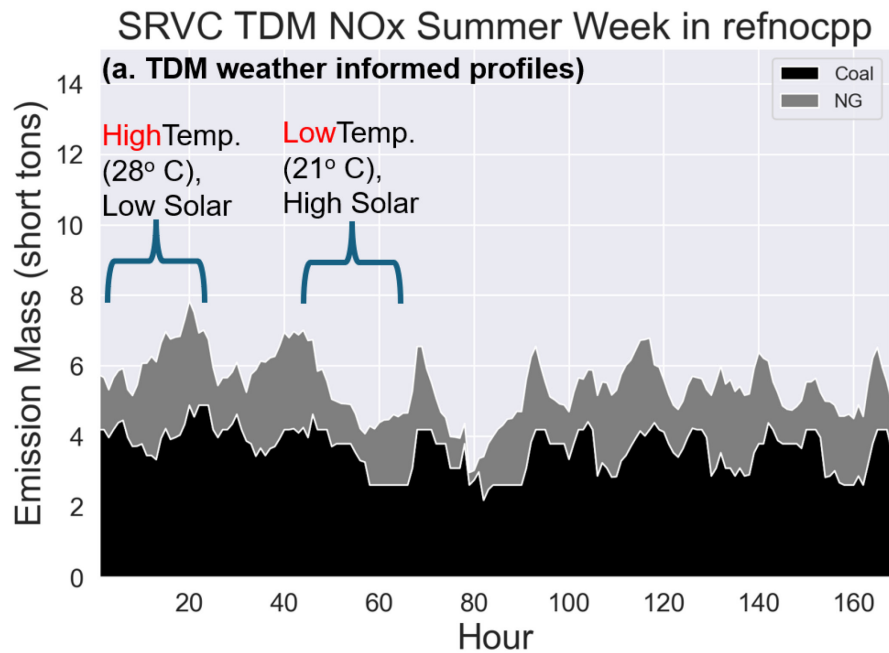
275 As discussed in the next three subsections below, many of the differences in emissions patterns arise  
276 from the interactions of weather and particulars of the generation mix, which are captured by the hourly  
277 TDM method but not the commonly used [SMOKE](#) downscaling method.

### 278 **3.2 TDM vs [SMOKE](#): Comparison of Emission Profiles**

279 Figure 4 focuses on comparing the diurnal patterns of NO<sub>x</sub> emissions profiles obtained using the TDM  
280 method and the [SMOKE](#) default method. It represents the hourly emissions of one week in the summer  
281 season for the 2050 projection. In Figure 4a, we can observe that the NO<sub>x</sub> variation patterns are correlated  
282 with weather. For example, comparing the first day (high temperature and low solar radiation) with the  
283 third day (low temperature and strong solar radiation), we can see a higher demand on the first day and a  
284 gradually increased NO<sub>x</sub> emission during the afternoon (due to thermal plants gradually ramping up to  
285 compensate for decreasing solar power). In contrast, the third day has a lower demand but a duck-curve-  
286 like NO<sub>x</sub> emissions profile (due to strong solar production replacing thermal plant operation in the after-  
287 noon). The TDM simulated profile is the result of system operation informed by impacts of weather on load  
288 demand and renewable energy production.

289 However, the [SMOKE](#) profile only relies on historical operation patterns based on generation mixes  
290 dominated by thermal power plants, whose day-to-day patterns emission are less affected by weather than  
291 renewable-dominated systems that have thermal plants as back-up. As shown in Figure 4b, the correspond-  
292 ing [SMOKE](#) NO<sub>x</sub> profile has a repeating and simple pattern mimicking the traditional operation of thermal  
293 power system, ignoring the impacts of weather on power system operation. The peak emission occurs  
294 around noon every day at the same time as peak load demand. However, this is no longer accurate for a  
295 power system with a large amount of solar where the timing of peak emission is postponed to later afternoon  
296 around 7-8 pm. The timing of power emission is significant because the reaction and transport of air pollu-  
297 tants and formation of secondary air pollutants are highly correlated with when pollutants are emitted into  
298 the atmosphere and the local weather conditions. Therefore, the emission profile based on the historical

299 power operations may be inappropriate for a future clean power system with a large amount of variable  
300 renewable energy, especially in the context of climate change where the impacts of weather information  
301 should be considered for more accurate estimates of power operation and emissions.



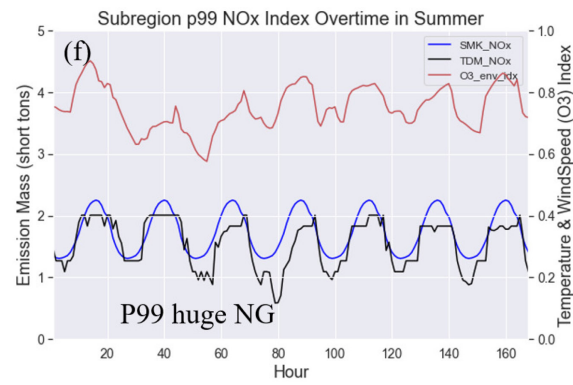
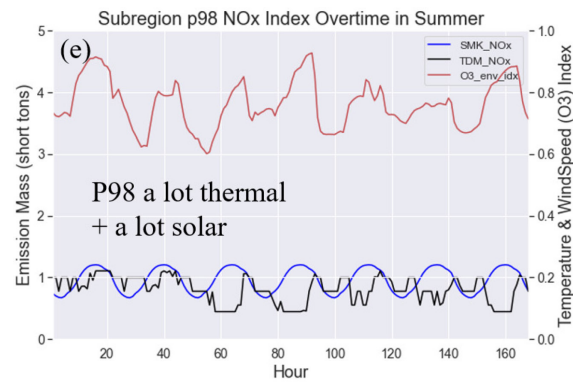
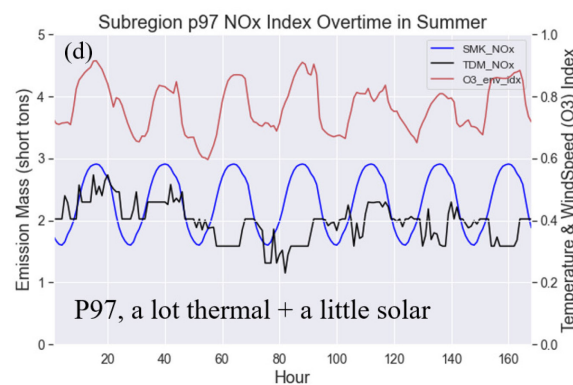
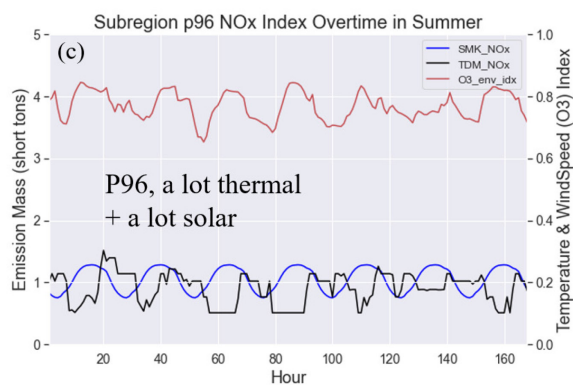
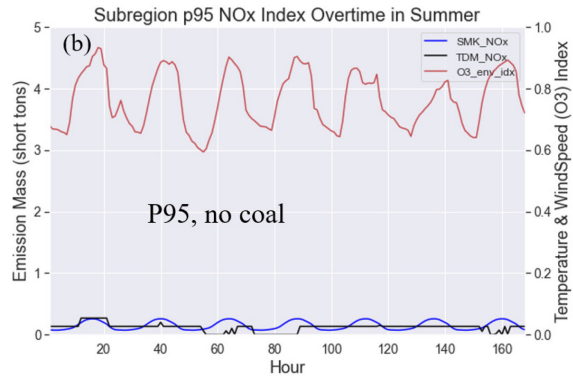
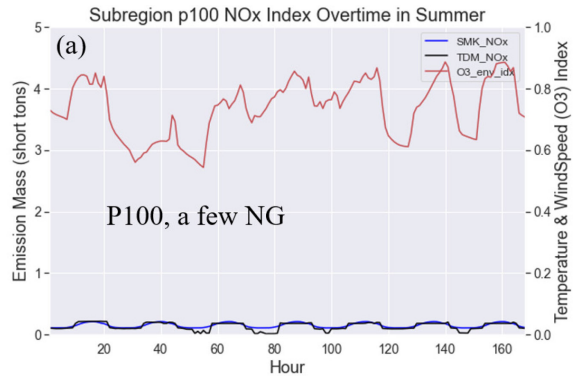
304 Figure 4. Hourly NO<sub>x</sub> emission profiles in summer week in region SRVC in scenario refnocpp (a. TDM  
305 downscaling; b. SMOKE default profile)

306

307 **3.3 TDM vs SMOKE: Weather Indices**

308 To illustrate the influence of weather information on pollutant formation, we develop a simple index of  
309 the meteorological potential for tropospheric O<sub>3</sub> formation [59], [60] and analyze its covariation with NO<sub>x</sub>  
310 emission profiles of TDM and SMOKE at the subregion level in Figure 5. The O<sub>3</sub> formation index is cal-  
311 culated as an equally weighted sum of a 0-1 rescaled wind speed and a 0-1 rescaled solar radiation, where  
312 a higher value of the O<sub>3</sub> index for a given hour indicates a greater risk of O<sub>3</sub> formation-favorable weather  
313 conditions characterized by low wind speed and high solar radiation. When the peak time of power emis-  
314 sion coincides with a high value of the O<sub>3</sub> index, there could be a higher risk of forming secondary O<sub>3</sub> in  
315 the atmosphere.

316 Comparing subregions, we can expect a variety of patterns of local power NO<sub>x</sub> emissions and their  
317 relationship of local weather conditions because of their different generation mixes. In Figures 5a and 5b,  
318 subregions p100 and p95 are unlikely to be exposed to secondary O<sub>3</sub> from the local power system due to  
319 low levels of power NO<sub>x</sub> emissions. On the other hand, subregions p96 and p98 (Figure 5c and 5e) have a  
320 similar generation mix with large amounts of thermal plants and a significant amount of solar energy, which  
321 suggests that weather conditions may interact strongly with power resource operation in these areas. From  
322 Figures 5c and e, we observe a strong correlation between the resulting SMOKE NO<sub>x</sub> emission profile (blue  
323 curve) and O<sub>3</sub> index, particularly during peak hours when NO<sub>x</sub> emission and O<sub>3</sub> index are both at their  
324 maximum. In contrast, the resulting TDM profile (black curve) shows an opposite trend, with lower NO<sub>x</sub>  
325 emissions when the O<sub>3</sub> index is at its peak, which reflects the impacts of solar penetration on the operation  
326 of thermal plants, leading to postponed peak emissions hours. Meanwhile, in p97 (Figure 5d), a similar  
327 phenomenon can be observed on some days, except for the first two days of the week, although there is  
328 only a relatively small amount of solar power in the local generation mix. This contradiction implies that  
329 using the SMOKE profile for a system with high solar penetration could result in overestimating O<sub>3</sub> con-  
330 centrations in air quality simulations compared to using a profile generated by a TDM method, with the  
331 latter providing a more trustworthy estimate of the risk of O<sub>3</sub> penetration due to the changing operation of  
332 future power systems. Finally, in p99 (Figure 5f), because the local generation mix is purely dominated by  
333 thermal plants with limited renewable penetration, both the SMOKE profile and TDM results can correctly  
334 represent emissions patterns in such a case.



338 Figure 5. Hourly NO<sub>x</sub> emission profiles and O<sub>3</sub> formation index in summer week in subregions of SRVC  
 339 in refnocc (a. P100; b. P95; c. P96; d. P97; e. P98; f. P99)

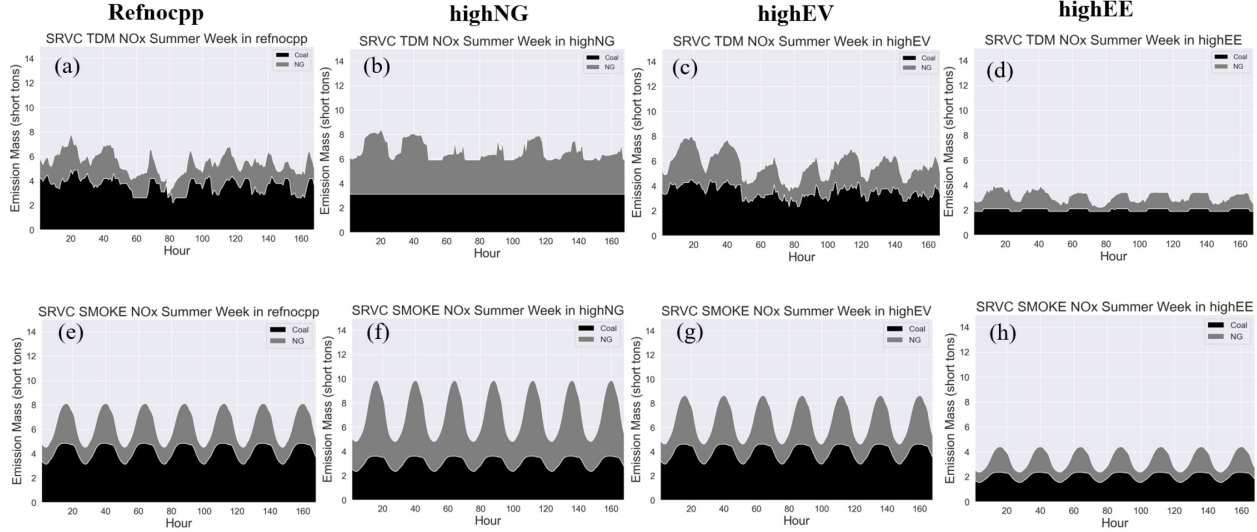
340

### 3.4 TDM vs SMOKE: Scenarios

342 In this section, we compare TDM and SMOKE NO<sub>x</sub> emissions in summer (Figure 6) and winter (Figure  
 343 7) weeks under different scenarios. The TDM profiles in summer exhibit diverse NO<sub>x</sub> emission patterns  
 344 and levels across the scenarios. The refnocc case and the highEV case share a similar (and highly variable)  
 345 TDM NO<sub>x</sub> pattern, reflecting the influence of gas and solar operations during the daytime. Their pattern is  
 346 distinct from the corresponding SMOKE profile whose diurnal pattern is the same every day. In contrast,

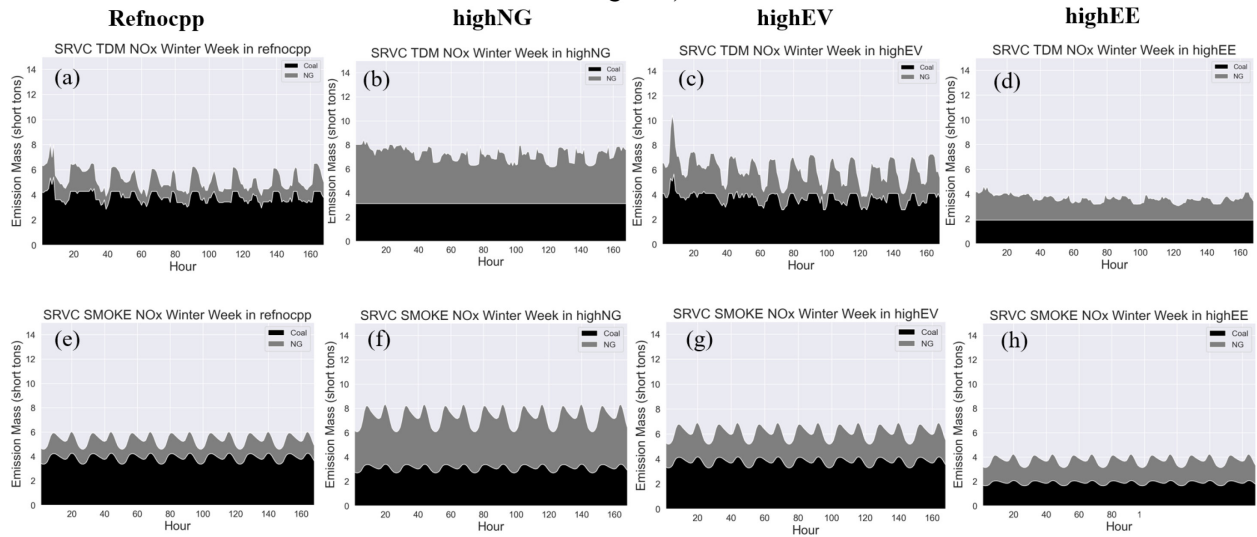
347 the highEE and highNG cases include more conventional thermal units, leading to different NO<sub>x</sub> emissions  
348 compared to refnocc and highEV cases. The highEE TDM pattern closely resembles the **SMOKE** pattern,  
349 suggesting that the **SMOKE** profile can sometimes suffice for simulating power emissions if the future  
350 system configuration does not shift towards greater reliance on variable renewable energy. In the highNG  
351 case, however, the TDM pattern appreciably deviates from the **SMOKE** pattern despite being dominated  
352 by thermal plants. This is due to the presence of a large amount of gas generation, which flattens the peak  
353 emissions of coal plants and shifts emissions to non-peak periods, resulting in an overall different emissions  
354 pattern compared to the **SMOKE** profile. Also, the highNG scenario shows approximately 25% fewer daily  
355 peak emissions, and 15% higher non-peak emissions compared to **SMOKE**. By comparing the profiles  
356 among different scenarios, we see that the TDM profiles provide plausible estimates of changes in system  
357 operation and emission patterns under different scenarios. In contrast, the **SMOKE** profiles exhibit implau-  
358 sibly similar emission patterns across the scenarios, with differences only in the total emissions levels.  
359 **SMOKE** profiles tend to misrepresent emission profiles, basing them on increasingly irrelevant historical  
360 patterns.

361 Compared to summer patterns, the differences between the TDM and **SMOKE** profiles in winter are  
362 less pronounced (Figure 7). The winter **SMOKE** profiles exhibit two daily peaks and account for the impacts  
363 of solar and load demand changes, which are generally similar to the TDM profile patterns. However, dif-  
364 ferences still exist in the accuracy of representing peaks and fluctuations across days. For instance, in the  
365 refnocc and highEE scenarios, the extreme peaks observed in the TDM profile on the first day are  
366 smoothed out by the **SMOKE** profiles when averaged over the remaining days. Furthermore, **SMOKE** pro-  
367 files may show distinctive daily fluctuation patterns compared to the TDM profile, with **SMOKE** being  
368 more variable than the TDM profile in the highEE or highNG scenarios, while being less so in the refnocc  
369 or highEV scenarios. Therefore, although the winter **SMOKE** profile is more realistic, it fails to capture the  
370 detailed changes in peaks and variations that the TDM profile can capture, which could significantly impact  
371 air quality simulations.



372

373 Figure 6. Hourly NO<sub>x</sub> emission in summer week of SRVC (a. TDM-refnocpp; b. TDM-highNG; c. TDM-  
 374 highEV; d. TDM-highEE; e. SMOKE-refnocpp; f. SMOKE-highNG; g. SMOKE-highEV; h. SMOKE-  
 375 highEE)



376

377 Figure 7. Hourly NO<sub>x</sub> emission in winter week of SRVC (a. TDM-refnocpp; b. TDM-highNG; c. TDM-  
 378 highEV; d. TDM-highEE; e. SMOKE-refnocpp; f. SMOKE-highNG; g. SMOKE-highEV; h. SMOKE-  
 379 highEE)

#### 380 4. Discussion

381 In this paper, we have introduced a novel fundamentals-based temporal downscaling method called the  
 382 Temporal Dispatch Model. TDM is a procedure for translating temporally aggregated emission results from  
 383 aggregate electric power sector models, such as NEMS, to the detailed plant-level hourly inputs required  
 384 by air pollutant simulation models, such as the emissions processing model SMOKE. TDM, when paired  
 385 with the Site-and-Grow (SAG) method in [49], develops spatially and temporally granular emissions pro-  
 386 jections under a given future technology and policy scenario. Because TDM captures the rich detail of the

387 power networks and generation technology in its dispatch model, the downscaled system's generation mix  
388 and operations at the subregional level not only reflect the scenario-specific fundamental structural changes  
389 in power systems resulting from a scenario's various technologic, economic, and weather drivers, but also  
390 reveals the spatial and temporal heterogeneity in system operations and emissions among those scenarios.

391 As a numerical case study, we made a comprehensive comparison of the proposed temporal downscal-  
392 ing method TDM with traditional **SMOKE** profile-based downscaling in the SRVC region power system  
393 of the NEMS model. We consider various aspects of the results, including resulting power emission pro-  
394 files, correlations with weather indices, and consistency with scenario information. The findings reveal that  
395 the TDM emissions profiles effectively capture how system operations respond to the impacts of weather  
396 on demand and renewable energy production patterns. In contrast, **SMOKE** profiles, which are based on  
397 historical operations, were found to be potentially biased and unresponsive to changes in the pattern of  
398 dispatch when representing future power emissions, particularly in the context of climate change and re-  
399 newables expansion. Furthermore, our analysis of **smog season** weather indices (representing meteorolog-  
400 ical conditions such as wind speed and solar radiation that favor O<sub>3</sub> formation) indicates that relying on the  
401 **SMOKE** NO<sub>x</sub> emission profile could lead to an overestimation of O<sub>3</sub> concentrations for a system that has  
402 relatively higher penetration of solar capacity. This overestimation is attributed to **SMOKE**'s misrepresen-  
403 tation of the timing of peak emissions relative to their occurrence in the presence of solar generation. TDM  
404 shifts emissions to the morning and evening peak demand periods due to mid-day solar energy production,  
405 which we conjecture would lessen the potential for tropospheric O<sub>3</sub> formation [61]. Finally, our analysis of  
406 four policy scenarios demonstrates that the **SMOKE** profiles exhibited no discernible differences in emis-  
407 sion patterns timing across the scenarios, only differences in their integrals (total emission levels). This  
408 inflexibility may result in an understatement of the impact of different scenarios on system operations and  
409 power emissions, particularly during the summer. In contrast, the TDM profiles result in more credible  
410 changes in system operation, variations in emission patterns, and timing of peak emissions that can be  
411 causally linked to weather patterns.

412 In summary, while GIP-**SMOKE** methods provide relatively quick assessments, they may introduce  
413 biases due to oversimplified emission patterns that fail to capture the dynamics of the energy transition, or  
414 insufficient consideration of uncertainties and complex interactions. As a result, these methods can anchor  
415 on historical emission patterns and average trends. In contrast, SAG-TDM methods are generally more  
416 responsive to policy and technology trends and better model system responses to weather. Thus, the SAG-  
417 TDM approach provide a more nuanced description of evolving emissions, better reflecting the distinctive  
418 characteristics and greater variability of renewable-based systems.

419 While the SAG-TDM downscaling method offers several advantages over traditional GIP-**SMOKE**  
420 approaches and is better suited for capturing the evolving characteristics of future power systems and

421 emissions, it does come with a tradeoff. The implementation of SAG-TDM introduces an increased com-  
422 putational burden and adds complexity to the modeling framework. Consequently, for future research, we  
423 recommend conducting quantitative analyses and comparisons of air quality simulations and their ultimate  
424 human health impacts using emission scenarios generated by both the SAG-TDM and GIP- **SMOKE** meth-  
425 ods. In particular, that method introduces additional complexity and requires additional model setup and  
426 coding effort. To apply SAG-TDM downscaling, researchers must convert the boundary conditions from  
427 the chosen aggregate model into the fine-grained in-puts required for the SAG-TDM model while main-  
428 taining consistency with assumptions about local power markets and policies. External data may also be  
429 needed to capture finer features or dynamics that are not present in the aggregate model. However, although  
430 more effort is needed for model and data development, computational speed becomes less of a concern (the  
431 difference in computation time between the two methods is typically within an hour in our experience).  
432 Altogether, this suggests that GIP-SMOKE may be preferable for policy makers needing quick, high-level  
433 insights when policy development timelines are tight. However, once the SAG-TDM model capability is  
434 developed, it will offer more detailed insights on locality-specific impacts to inform more extended and  
435 detailed policy processes.

436 Therefore, for future research, we first recommend conducting quantitative analyses and comparisons  
437 of air quality simulations and their ultimate human health impacts using emission scenarios generated by  
438 both the SAG-TDM and GIP-**SMOKE** methods. This comparative analysis could focus on evaluating the  
439 accuracy of results, computational efficiency, and identifying which methods are suited to various applica-  
440 tions. Furthermore, validating downscaled results is essential. Future work could involve comparing histor-  
441 ical simulation data with real-world observations (e.g., EPA CEMS data) to ensure accuracy. Lastly, we  
442 suggest additional applications, especially studies addressing equity issues in the energy transition process  
443 to assess how the benefits of overall emissions decreases are distributed. And for rapidly growing econo-  
444 mies where coal generation will likely continue to dominate in coming years, fine-grained downscaling  
445 methods can address impacts of policies such as those in China that have emphasized conversion to natural  
446 gas in urban areas.

#### 447 **Support Information**

448 Additional literature review on downscaling methods, model, data and processing methods, and addi-  
449 tional simulation results and analysis for power system operations.

#### 450 **Acknowledgment**

451 This article was developed under Assistance Agreement No. RD835871 awarded by the U.S. Environ-  
452 mental Protection Agency to Yale University. It has not been formally reviewed by EPA. The views ex-  
453 pressed in this document are solely those of the authors and do not necessarily reflect those of the Agency.  
454 EPA does not endorse any products or commercial services mentioned in this publication.

455 We thank Kai Wang and Yang Zhang of Northeastern University for meteorological simulations and  
456 SMOKE model runs; Leyang Feng of JHU for time series data processing; Pei Huang, Stephanie Weber,  
457 and Ken Gillingham of Yale University for developing the Yale-NEMS model and the policy scenarios.

## 458 **References**

459 [1] “Paris Agreement,” in Report of the Conference of the Parties to the United Nations Framework Con-  
460 vention on Climate Change. December, 2015, p. 2017.

461 [2] Schleussner, C.F., Rogelj, J., Schaeffer, M., Lissner, T., Licker, R., Fischer, E.M., Knutti, R., Lever-  
462 mann, A., Frieler, K. and Hare, W., “Science and policy characteristics of the Paris Agreement tem-  
463 perature goal,” *Nat. Clim. Change*, vol. 6, no. 9, pp. 827–835, 2016.

464 [3] “FACT SHEET: President Biden to Catalyze Global Climate Action through the Major Economies  
465 Forum on Energy and Climate,” The White House. Accessed: Jun. 17, 2023. Available:  
466 [https://www.whitehouse.gov/briefing-room/statements-releases/2023/04/20/fact-sheet-president-  
467 biden-to-catalyze-global-climate-action-through-the-major-economies-forum-on-energy-and-climate/](https://www.whitehouse.gov/briefing-room/statements-releases/2023/04/20/fact-sheet-president-biden-to-catalyze-global-climate-action-through-the-major-economies-forum-on-energy-and-climate/)

468 [4] Rogelj, J., Geden, O., Cowie, A. and Reisinger, A., “Three ways to improve net-zero emissions tar-  
469 gets,” *Nature*, vol. 591, no. 7850, pp. 365–368, 2021.

470 [5] H. Ritchie, M. Roser, and P. Rosado, “CO<sub>2</sub> and Greenhouse Gas Emissions,” Our World Data, May  
471 2020, Available: <https://ourworldindata.org/emissions-by-sector>

472 [6] Bouckaert, S., Pales, A.F., McGlade, C., Remme, U., Wanner, B., Varro, L., D'Ambrosio, D. and Spen-  
473 cer, T., “Net zero by 2050: A roadmap for the global energy sector,” 2021.

474 [7] Jaeger, B. and Machry, P., “Energy transition and challenges for the 21st century,” IUGGSMUIN  
475 Model U. N., vol. 2, pp. 337–374, 2014.

476 [8] Davis, S.J., Lewis, N.S., Shaner, M., Aggarwal, S., Arent, D., Azevedo, I.L., Benson, S.M., Bradley,  
477 T., Brouwer, J., Chiang, Y.M. and Clack, C.T., “Net-zero emissions energy systems,” *Science*, vol.  
478 360, no. 6396, 2018.

479 [9] Edenhofer, O., Climate change 2014: mitigation of climate change, vol. 3. Cambridge University Press,  
480 2015.

481 [10] Carley, S. and Konisky, D. M., “The justice and equity implications of the clean energy transition,”  
482 *Nat. Energy*, vol. 5, no. 8, pp. 569–577, 2020.

483 [11] Carley, S., Evans, T.P., Graff, M. and Konisky, D.M., “A framework for evaluating geographic dispar-  
484 ities in energy transition vulnerability,” *Nat. Energy*, vol. 3, no. 8, pp. 621–627, 2018.

485 [12] Shen, G., Ru, M., Du, W., Zhu, X., Zhong, Q., Chen, Y., Shen, H., Yun, X., Meng, W., Liu, J. and  
486 Cheng, H., “Impacts of air pollutants from rural Chinese households under the rapid residential energy  
487 transition,” *Nat. Commun.*, vol. 10, no. 1, p. 3405, 2019.

488 [13]Hanson, G. H., “Local Labor Market Impacts of the Energy Transition: Prospects and Policies,” Na-  
489 tional Bureau of Economic Research, 2023.

490 [14]Raimi, D., Carley, S. and Konisky, D., “Mapping county-level vulnerability to the energy transition in  
491 US fossil fuel communities,” *Sci. Rep.*, vol. 12, no. 1, p. 15748, 2022.

492 [15]Pereira, G., Bell, M.L., Honda, Y., Lee, J.T., Morawska, L. and Jalaludin, B., “Energy transitions, air  
493 quality and health,” *Environ. Res. Lett.*, vol. 16, no. 2, p. 020202, 2021.

494 [16]Bistline, J., Blanford, G., Brown, M., Burtraw, D., Domeshek, M., Farbes, J., Fawcett, A., Hamilton,  
495 A., Jenkins, J., Jones, R. and King, B., “Emissions and energy impacts of the Inflation Reduction Act,”  
496 *Science*, vol. 380, no. 6652, pp. 1324–1327, Jun. 2023, doi: 10.1126/science.adg3781.

497 [17] Nalley, S. and LaRose, A., “Annual energy outlook 2022,” *Energy Inf. Agency*, p. 23, 2022.

498 [18]Calvin, K., Patel, P., Clarke, L., Asrar, G., Bond-Lamberty, B., Cui, R.Y., Di Vittorio, A., Dorheim,  
499 K., Edmonds, J., Hartin, C. and Hejazi, M., “GCAM v5. 1: representing the linkages between energy,  
500 water, land, climate, and economic systems,” *Geosci. Model Dev.*, vol. 12, no. 2, pp. 677–698, 2019.

501 [19]Appel, K.W., Napelenok, S.L., Foley, K.M., Pye, H.O., Hogrefe, C., Luecken, D.J., Bash, J.O., Roselle,  
502 S.J., Pleim, J.E., Foroutan, H. and Hutzell, W.T., “Description and evaluation of the Community Mul-  
503 tiscale Air Quality (CMAQ) modeling system version 5.1,” *Geosci. Model Dev.*, vol. 10, no. 4, pp.  
504 1703–1732, 2017.

505 [20]Peckham, S. E., “WRF/Chem version 3.3 user’s guide,” 2012.

506 [21]Tessum, C.W., Hill, J.D. and Marshall, J.D., “InMAP: A model for air pollution interventions,” *PloS*  
507 *One*, vol. 12, no. 4, p. e0176131, 2017.

508 [22]Chalal, M.L., Medjdouba, B., Whitea, M. and Shrahilya, R., “Energy planning and forecasting ap-  
509 proaches for supporting physical improvement strategies in the building sector: A review,” *Renew.*  
510 *Sustain. Energy Rev.*, vol. 64, pp. 761–776, 2016.

511 [23]Perugu, H., “Emission modelling of light-duty vehicles in India using the revamped VSP-based  
512 MOVES model: The case study of Hyderabad,” *Transp. Res. Part Transp. Environ.*, vol. 68, pp. 150–  
513 163, 2019.

514 [24]Brown, M., Cole, W., Eurek, K., Becker, J., Bielen, D., Chernyakhovskiy, I., Cohen, S., Frazier, A.,  
515 Gagnon, P., Gates, N. and Greer, D., “Regional energy deployment system (ReEDS) model documen-  
516 tation: version 2019,” National Renewable Energy Lab.(NREL), Golden, CO, 2020.

517 [25] Capuano, L., “Annual energy outlook 2019,” *Wash. DC US Energy Inf. Adm.*, 2019.

518 [26]Ekström, M., Grose, M. R., and Whetton, P. H., “An appraisal of downscaling methods used in climate  
519 change research,” *Wiley Interdiscip. Rev. Clim. Change*, vol. 6, no. 3, pp. 301–319, 2015.

520 [27] Gonzalez-Aparicio, I., Monforti, F., Volker, P., Zucker, A., Careri, F., Huld, T. and Badger, J., “Sim-  
521 ulating European wind power generation applying statistical downscaling to reanalysis data,” *Appl.*  
522 *Energy*, vol. 199, pp. 155–168, 2017.

523 [28] Wilby, R. L., Charles, S. P., Zorita, E., Timbal, B., Whetton, P. and Mearns, L. O., “Guidelines for use  
524 of climate scenarios developed from statistical downscaling methods,” *Support. Mater. Intergov. Panel*  
525 *Clim. Change Available DDC IPCC TGCIA*, vol. 27, 2004.

526 [29] Y.-H. Ahn, J.-H. Woo, F. Wagner, and S. J. Yoo, “Downscaled energy demand projection at the local  
527 level using the Iterative Proportional Fitting procedure,” *Appl. Energy*, vol. 238, pp. 384–400, 2019.

528 [30] E. H. Girvetz, E. P. Maurer, P. B. Duffy, A. Ruesch, B. Thrasher, and C. Zganjar, “Making climate  
529 data relevant to decision making: the important details of spatial and temporal downscaling,” 2013.

530 [31] Ralston Fonseca, F., Craig, M., Jaramillo, P., Bergés, M., Severnini, E., Loew, A., Zhai, H., Cheng, Y.,  
531 Nijssen, B., Voisin, N. and Yearsley, J. “Effects of climate change on capacity expansion decisions of  
532 an electricity generation fleet in the Southeast US,” *Environ. Sci. Technol.*, vol. 55, no. 4, pp. 2522–  
533 2531, 2021.

534 [32] Buster, G., Rossol, M., Maclaurin, G., Xie, Y. and Sengupta, M., “A physical downscaling algorithm  
535 for the generation of high-resolution spatiotemporal solar irradiance data,” *Sol. Energy*, vol. 216, pp.  
536 508–517, 2021.

537 [33] Losada Carreño, I., Craig, M.T., Rossol, M., Ashfaq, M., Batibeniz, F., Haupt, S.E., Draxl, C., Hodge,  
538 B.M. and Brancucci, C., “Potential impacts of climate change on wind and solar electricity generation  
539 in Texas,” *Clim. Change*, vol. 163, pp. 745–766, 2020.

540 [34] F. Giorgi, “Regionalization of climate change information for impact assessment and adaptation,” *Bull.*  
541 *World Meteorol. Organ.*, vol. 57, no. 2, pp. 86–92, 2008.

542 [35] D. P. van Vuuren, S. J. Smith, and K. Riahi, “Downscaling socioeconomic and emissions scenarios for  
543 global environmental change research: a review,” *Wiley Interdiscip. Rev. Clim. Change*, vol. 1, no. 3,  
544 pp. 393–404, 2010.

545 [36] Y. Xue, Z. Janjic, J. Dudhia, R. Vasic, and F. De Sales, “A review on regional dynamical downscaling  
546 in intraseasonal to seasonal simulation/prediction and major factors that affect downscaling ability,”  
547 *Atmospheric Res.*, vol. 147, pp. 68–85, 2014.

548 [37] L. Ran, D. H. Loughlin, D. Yang, Z. Adelman, B. H. Baek, and C. G. Nolte, “ESP v2. 0: enhanced  
549 method for exploring emission impacts of future scenarios in the United States—addressing spatial al-  
550 location,” *Geosci. Model Dev. Discuss.*, vol. 8, no. 1, pp. 263–300, 2015.

551 [38] D. H. Loughlin, W. G. Benjey, and C. G. Nolte, “ESP v1. 0: methodology for exploring emission  
552 impacts of future scenarios in the United States,” *Geosci. Model Dev.*, vol. 4, no. 2, pp. 287–297, 2011.

553 [39] Hobbs, B.F., Hu, M.C., Chen, Y., Ellis, J.H., Paul, A., Burtraw, D. and Palmer, K.L. “From regions to  
554 stacks: spatial and temporal downscaling of power pollution scenarios,” *IEEE Trans. Power Syst.*, vol.  
555 25, no. 2, pp. 1179–1189, 2010.

556 [40] Chen, Y., Hobbs, B.F., Ellis, J.H., Crowley, C. and Joutz, F., “Impacts of climate change on power  
557 sector NO<sub>x</sub> emissions: A long-run analysis of the US mid-atlantic region,” *Energy Policy*, vol. 84, pp.  
558 11–21, 2015.

559 [41] Benjey, W., Houyoux, M. and Susick “Implementation of the SMOKE emission data processor and  
560 SMOKE tool input data processor in models-3,” US EPA, 2001.

561 [42] Craig, M.T., Jaramillo, P., Hodge, B.M., Nijssen, B. and Brancucci, C., “Compounding climate change  
562 impacts during high stress periods for a high wind and solar power system in Texas,” *Environ. Res.  
563 Lett.*, vol. 15, no. 2, p. 024002, 2020.

564 [43] Bistline J., “Variability in deeply decarbonized electricity systems,” *Environ. Sci. Technol.*, vol. 55,  
565 no. 9, pp. 5629–5635, 2021.

566 [44] Auffhammer, M., Baylis, P. and Hausman, C.H., “Climate change is projected to have severe impacts  
567 on the frequency and intensity of peak electricity demand across the United States,” *Proc. Natl. Acad.  
568 Sci.*, vol. 114, no. 8, pp. 1886–1891, 2017.

569 [45] Yalew, S.G., van Vliet, M.T., Gernaat, D.E., Ludwig, F., Miara, A., Park, C., Byers, E., De Cian, E.,  
570 Piontek, F., Iyer, G. and Mouratiadou, I., “Impacts of climate change on energy systems in global and  
571 regional scenarios,” *Nat. Energy*, vol. 5, no. 10, pp. 794–802, 2020.

572 [46] Levin, T., Botterud, A., Mann, W.N., Kwon, J. and Zhou, Z., “Extreme weather and electricity markets:  
573 Key lessons from the February 2021 Texas crisis,” *Joule*, vol. 6, no. 1, pp. 1–7, 2022.

574 [47] Hendriks, C., Kuenen, J., Kranenburg, R., Scholz, Y. and Schaap, M., “A shift in emission time profiles  
575 of fossil fuel combustion due to energy transitions impacts source receptor matrices for air quality,”  
576 *Environ. Sci. Process. Impacts*, vol. 17, no. 3, pp. 510–524, 2015.

577 [48] Ralston Fonseca, F., Jaramillo, P., Bergés, M. and Severnini, E., “Seasonal effects of climate change  
578 on intra-day electricity demand patterns,” *Clim. Change*, vol. 154, pp. 435–451, 2019.

579 [49] Wang, S., Fisher, E.B., Feng, L., Zhong, X., Ellis, J.H. and Hobbs, B.F., “Linking energy sector and  
580 air quality models through downscaling: Long-run siting of electricity generators to account for spatial  
581 variability and technological innovation,” *Sci. Total Environ.*, vol. 772, p. 145504, 2021.

582 [50] Hobbs, B.F., Drayton, G., Fisher, E.B. and Lise, W., “Improved transmission representations in oligo-  
583 politistic market models: quadratic losses, phase shifters, and DC lines,” *IEEE Trans. Power Syst.*,  
584 vol. 23, no. 3, pp. 1018–1029, 2008.

585 [51] Bothwell, C. D. and Hobbs, B. F., “How Sampling and Averaging Historical Solar and Wind Data Can  
586 Distort Resource Adequacy”, *IEEE Trans. Sus. Energy*, 14, no. 3 1337-1345. 2022.

587 [52]Collins, S., Deane, P., Gallachóir, B.Ó., Pfenninger, S. and Staffell, I., “Impacts of Inter-annual Wind  
588 and Solar Variations on the European Power System” Joule 2.10, 2076-2090, 2018.

589 [53]M. Houyoux, J. Vukovich, J. E. Brandmeyer, C. Seppanen, and A. Holland, “Sparse matrix operator  
590 kernel emissions modeling system-SMOKE User manual,” Cent. Environ. Programs Res. Triangle  
591 Park NC, 2000.

592 [54]US EPA, “FACT SHEET: Overview of the Clean Power Plan.”, Available: <https://archive.epa.gov/epa/cleanpowerplan/fact-sheet-overview-clean-power-plan.html>

593 [55]Gillingham, K. and Huang, P., “Is abundant natural gas a bridge to a low-carbon future or a dead-end?,”  
594 Energy J., vol. 40, no. 2, 2019.

595 [56]Wolfram, P., Weber, S., Gillingham,K., and Hertwich, E. G., “Pricing indirect emissions accelerates  
596 low—carbon transition of US light vehicle sector,” Nat. Commun., vol. 12, no. 1, p. 7121, 2021.

597 [57]Gillingham, K. T., Huang, P., Buehler,C., Peccia, J. and Gentner, D. R., “The climate and health ben-  
598 efits from intensive building energy efficiency improvements,” Sci. Adv., vol. 7, no. 34, p. eabg0947,  
599 2021.

600 [58]Short, W., Sullivan, P., Mai, T., Mowers, M., Uriarte, C., Blair, N., Heimiller, D. and Martinez, A.,  
601 “Regional energy deployment system (ReEDS),” National Renewable Energy Lab.(NREL), Golden,  
602 CO, 2011.

603 [59]Lelieveld, J. and Dentener, F. J., “What controls tropospheric ozone?,” J. Geophys. Res. Atmospheres,  
604 vol. 105, no. D3, pp. 3531–3551, 2000, doi: 10.1029/1999JD901011.

605 [60]Trainer, M., Parrish, D.D., Goldan, P.D., Roberts, J. and Fehsenfeld, F.C., “Review of observation-  
606 based analysis of the regional factors influencing ozone concentrations,” Atmos. Environ., vol. 34, no.  
607 12, pp. 2045–2061, Jan. 2000, doi: 10.1016/S1352-2310(99)00459-8.

608 [61]Seinfeld J. H., and Pandis, S. N., Atmospheric Chemistry and Physics: From Air Pollution to Climate  
609 Change. John Wiley & Sons, 2016.

610 [62]Ebrahimi, S., Mac Kinnon, M. and Brouwer, J., “California end-use electrification impacts on carbon  
611 neutrality and clean air.” Applied Energy 435-449, 2018.

612 [63]Forrest, K., Lane, B., Tarroja, B., Mac Kinnon, M. and Samuelsen, S., “Emissions and air quality im-  
613 plications of enabling on-road vehicles as flexible load through widescale zero emission vehicle de-  
614 ployment in California.” Transportation Research Record 2677.3: 1085-1096, 2023.

615 [64]Kerl, P.Y., Zhang, W., Moreno-Cruz, J.B., Nenes, A., Realff, M.J., Russell, A.G., Sokol, J. and  
616 Thomas, V.M., "New approach for optimal electricity planning and dispatching with hourly time- scale  
617 air quality and health considerations." PNAS, 112.35: 10884-10889, 2015.

618

619 [65] Geng, Z., Chen, Q., Xia, Q., Kirschen, D.S. and Kang, C., "Environmental generation scheduling con-  
620 sidering air pollution control technologies and weather effects." IEEE Trans. on Power Sys. 32.: 127-  
621 136, 2016.

622 [66] Razeghi, G., MacKinnon, M., Wu, K., Matthews, B., Zhu, S. and Samuelsen, S., "Air quality assess-  
623 ment of a mass deployment of microgrids." Sci. Total Environ. 947: 174632, 2024.